The development of a real-time flooding operation model in the Tseng-Wen Reservoir

Yu-Wen Chen, Jui-Pin Tsai, Liang-Cheng Chang, Chih-Chao Ho and You-Cheng Chen

ABSTRACT

Typhoon events occur frequently in Taiwan resulting in flood-related disasters. A well-operated reservoir can reduce the severity of a disaster. This study incorporates a genetic algorithm, a river hydraulic model, an artificial neural network and a simulation model of Tseng-Wen Reservoir to propose a real-time flooding operation model. The model includes two parts: an optimal flooding operation model (OFOM) and a reservoir inflow forecasting. Given an inflow condition, the OFOM is run based on the safety of the dam structure, reservoir flooding operation rule, and minimization of the downstream loss due to flood. A simple and robust model for reservoir inflow forecasting, which automatically chooses the most similar event from a typhoon event database as the future inflow, is developed. This study compares the model results with the real operations during Typhoons Sepat, Krosa, Kalmaegi, Fung-wong, Sinlaku, and Jangmi. This study compares the performances of the proposed model with the practical operation operated by the management center of Tseng-Wen Reservoir. The proposed model indicates shorter flooding duration in the downstream area. For example, the flood durations of the model output are 4 and 3 hours shorter during Typhoon Krosa and Sinlaku, respectively, than the practical operations.

Key words | artificial neural network, Hydrologic Engineering Centers River Analysis System (HEC-RAS), historical typhoon event database, real-time reservoir flooding operation model

Yu-Wen Chen
Jui-Pin Tsai
Liang-Cheng Chang (corresponding author)
You-Cheng Chen
Department of Civil Engineering,
National Chiao Tung University,
Hsinchu City 300,
Taiwan (ROC)
E-mail: *lcchang31938@gmail.com*

Chih-Chao Ho
Construction and Disaster Prevention Research Center,
Feng Chia University,
Taichung City 40724,
Taiwan

Liang-Cheng Chang
EB311,
1001 University Rd,
Hsinchu City,
Taiwan 300,
ROC

INTRODUCTION

During the summer season, typhoons release a tremendous amount of rainfall in Taiwan resulting in major natural disasters. Reservoirs adjust their releases in preparation for heavy rainfalls due to incoming typhoons. If the releases exceed the capacity of the downstream waterway in populated areas this can result in a significant loss of life. An area of increasing importance is to make optimal use of a reservoir to delay and decrease the peak flood flow in the downstream waterway, while maintaining a good storage for summer time water supplies. Developing Decision Support Systems (DSSs) for optimizing flood control of reservoirs has become an important issue.

DSSs that address optimal problems of reservoir operations normally can be stated with the objective to minimize flood damage in the downstream area and maximize the safety of the dam. The DDSs also are subject to constraints including physical laws governing the hydraulics of the systems and the operational constraints on reservoir releases and levels, and river stages at specified locations of the river-reservoir system (Ahmed & Mays 2013). Normally, simulation models such as rainfall-runoff models and river routing models are embedded in the DSSs to present the physical laws. The framework of the DSS is a kind of optimization/simulation model.

The main objective of flood control in most previous studies has normally been to minimize flood damage in the downstream area (Windsor 1973; Chang & Chen 1998; Hsu & Wei 2007; Malekmohammadi *et al*. 2010; Valeriano

doi: 10.2166/nh.2013.301

et al. 2010) and the decision variables are the release quantities of reservoirs. The flood damage can be presented in different forms such as the values of damage loss and the volumes or heights of river flow. Chang & Chen (1998) maximized the reduction in peak flow. Hsu & Wei (2007) minimized the peak heights at control points in the downstream area.

For multi-purpose flood control, some other sub-objects such as those for the purpose of water resource management are also added in the objective function with minor priorities. Chang & Chen (1998) maximized the increment of reservoir storage after flood operation. The increment of reservoir storage can become a water resource for the next drought season. Under similar concepts for water resource management, Valeriano *et al.* (2010) maximized the spare volumes of the reservoir. Hsu & Wei (2007) kept the reservoir water level at a pre-defined target after flood operation. At the early stage of a flood season, the targeted level should be lower for the preparation of flood operation for the next coming storm. At the end stage of a flood season, the target level should be higher for the purpose of water resource supply during the next drought season.

In the framework of an optimization/simulation model, the selection of the optimization algorithm is crucial. Labadie (2004) gave a great review for the optimal operation of multi-reservoir systems. Because the conservation of a reservoir system is linear, the simplex method of linear programming and its variants which can be solved efficiently become full of attraction for long-term operation of reservoir system models (Nash & Sofer 1996). Although the behavior of river routing might be nonlinear for the flood operation, linear programming still can be applied under linearization or linear simplification such as the Muskingum method. Windsor (1973), Needham *et al.* (2000) and Hsu & Wei (2007) applied linear programming based algorithms on their flood operation models.

Many reservoir system optimization problems such as the hydropower system and river complex river routing system cannot be realistically modeled using piecewise linearization, and must be attacked directly as nonlinear programming problems (Labadie 2004). Nonlinear programming, a kind of gradient-based algorithm, is traditionally applied in these problems. Unver & Mays (1990) and Ahmed & Mays (2013) developed models for real-time optimal flood operation of a river–reservoir system. These models combined a nonlinear programming algorithm with an unsteady flow flood-routing simulation model.

Both linear programming and nonlinear programming models are algorithmic procedures, meaning that well-structured, convergent solution processes are applied to quantitative information. Unlike most of the optimization algorithms, heuristic programs cannot guarantee termination to even local optimal solutions. These methods strive for acceptable or satisfying solutions, but they are often capable of achieving global optimal solutions to problems where traditional algorithmic methods would fail to converge or get stuck in local optima (Labadie 2004). The genetic algorithm (GA) which was firstly developed by Holland (1975) is a famous choice in the category of heuristic programs. Many researchers have applied the genetic algorithm and its variants to water resource management problems. Chang *et al.* (2009a) integrated a genetic algorithm and constrained differential dynamic programming on optimal expansion schedules of system capacity for groundwater supply. Chang *et al.* (2009b) applied a multi-objective genetic algorithm to analyze the conflict among different water use sectors during a drought period. Chang *et al.* (2010) and Hınçal *et al.* (2011) applied genetic algorithms for optimizing multi-use reservoir operation. Based on the above, the genetic algorithm and its variants is an attractive choice for solving optimization problems.

Physical laws such as the river routing are constraints in the DSSs of flood control. An unsteady flow simulator is required to predict the impacts of release quantities on the optimization of a river–reservoir system. For the implementation of river routing, Windsor (1973), Hsu & Wei (2007) and Wei & Hsu (2009) developed a river hydraulic model with the Muskingum method. This linear Muskingum equation was used to describe the linear relationship between reservoir release and stage at the control point. The calculation of the Muskingum method is efficient in the optimal model. However, its linear simplification between flow rate and water stage cannot be extended to solve complex flows directly. To avoid the limitation, Malekmohammadi *et al.* (2010) embedded a fully unsteady numerical model, HEC-RAS (Hydrologic Engineering Centers River Analysis System), to increase the accuracy of river routing for flooding operation. To increase the accuracy of river routing, the HEC-RAS model requires a greater time for calculation.

The artificial neural network (ANN) is a powerful tool from the field of data mining and has many applications in hydraulic related studies. Applying a well-trained ANN instead of a full function numerical model can greatly reduce the computational time and easily integrates with other algorithms, such as optimization and management models. Loke *et al.* (1997) applied an ANN model to simulate an urban drainage system with given rainfall data. To estimate the seasonal river flow, Sajikumar & Thandaveswara (1999) applied an ANN to develop the relationship between rainfall and river flow. Halff *et al.* (1993) and Lorrai & Sechi (1995) applied an ANN to model the relationship between watershed rainfall and surface runoff. Tayfur & Singh (2006) integrated Fuzzy logic, ANN, and kinematic wave theory to develop a rainfall-runoff model. For the application of modeling river hydraulics and surface runoff, ANN is the best option to increase the computational efficiency without linearization.

Flood management to control the rate of discharge in the river network after periods of heavy rainfall is a complex task (Delgoda *et al.* 2013). Approaches of DSSs for real-time operation of flooding control can be clustered into two categories. The first one is to simulate the entire horizon of the operation process of river–reservoir systems based on historical storm records or ensemble hyetographs and, then, flooding operation rules are concluded from the simulations (Alemu *et al.* 2010; Ahmed & Mays 2013). During a real-time operation, the DSSs can provide operation decisions based on the rule curves and current observations of precipitations or inflows. Because of climate change, the current characteristics of precipitation or inflow vary differently to the characteristics observed decades ago. Applying the decisions concluded from historical storm records or ensemble hyetographs might introduce high uncertainty due to the effect of climate change (Ahmed & Mays 2013; Delgoda *et al.* 2013).

The second one is to integrate an optimization/simulation model with a real-time forecast model for the future precipitations or inflows. The determination of the optimal decisions is based on the current observations and the future forecasts (Niewiadomska-Szynkiewicz *et al.* 1996; Hsu & Wei 2007) and the effect of climate change is widely considered in many forecast models. Niewiadomska-Szynkiewicz *et al.* (1996) apply a hierarchical decision mechanism and a predictive control algorithm on their real-time control model for a multi-reservoir system. The predictive control algorithm involves optimization of the control trajectory for a given prediction or forecast of external uncontrolled inputs. Hsu & Wei (2007) embed a quantitative precipitation forecast (QPF) model and a stream flow prediction model into a real-time operation model. The QPF model presents the statistical relationships between typhoon tracks and average precipitations. Based on the real-time observation of a typhoon track, the real-time operation model determines real-time releases of reservoirs. A forecast model of precipitation or inflow is an important element in a real-time operation (or control) model.

In the state-of-the-art for optimal operation of multi-reservoir systems, Labadie (2004) concludes that even with the presence of error, the use of forecasting of precipitation or inflow is preferable in real-time optimal control models. The quality of flow forecasting is often quantified in terms of lead time and accuracy. The lead time of the forecast is defined as the time interval between the issuing of the forecast and the time when the forecasted event is expected (Mays & Tung 2002). Zhao *et al.* (2013) indicate that forecast uncertainty evolves in real-time if forecasts can be dynamically updated. The uncertainties of forecasts for a certain time period decrease over time as more hydrologic information becomes available. Based on the above, a forecasting model which has the ability to assimilate its forecasting result is required in a real-time model for flood control.

This study proposes to develop a real-time flooding operation model (RTFOM) and the study area is the reservoir-river system which contains Tseng-Wen Reservoir and the downstream river. The proposed model simultaneously considers not only the impacts of flood damage control but also the future impact of water resource management. To evaluate the flood damage downstream, an ANN model, instead of the HEC-RAS model, was proposed. The training data of reservoir releases and the downstream river stage of Tseng-Wen River were simulated by the HEC-RAS model first. The ANN model can greatly increase the computational performance without linear assumptions. A genetic algorithm (GA) which has the ability to solve a nonlinear problem was used to determine the optimal flood releases. For the real-time operation, this study forecasts future inflow of the reservoir by comparing the observed

inflow hydrograph with historical data in the typhoon event database which is developed by the study. Although the concept of the forecasting is simple, the proposed approach has the ability to assimilate its forecasting result. As more observations become available, a similar typhoon pattern could be identified and the future inflow could be forecasted.

MODEL DEVELOPMENT

The RTFOM was developed in this study and included two parts: (1) Optimal Flooding Operation Planning Model (OFOPM) and (2) Typhoon Event Database (Figure 1). Given an inflow condition, the OFOPM integrated the surface runoff model, river hydraulic model, ANN, and GA to define the optimal release of the reservoir based on maintaining the safety of the dam structure, minimizing the downstream loss, and considering the current reservoir operation rule.

The Typhoon Event Database was developed by studying the historical inflow hydrograph records from 40 typhoon events. In the real-time operation, the operator compares the observed inflow data with the historical inflow hydrograph and forecasts the inflow by matching it with a historical typhoon event. As more observed data becomes available, the inflow forecasts improve in accuracy.

Optimal flooding operation planning model

The proposed model should simultaneously consider the reservoir storage at the end of a flood and its impact on the downstream river. The optimal formulations of the OFOPM are listed in Equations (1)–(9).

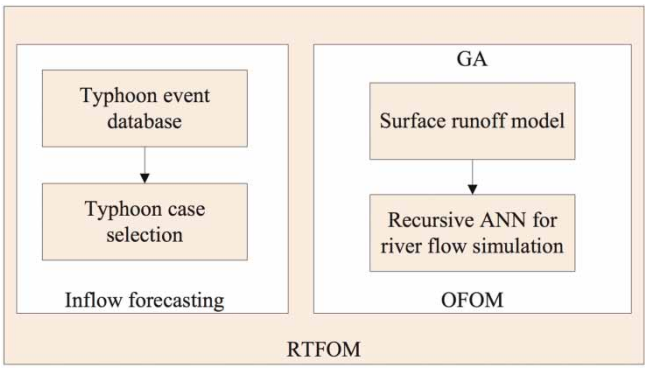

Figure 1 | The model architecture diagram for the RTFOM.

$$\min_{\vec{R}}\left\{\omega_1\frac{|S^{\text{target}}-S_{t_{III}}|}{S^{\text{target}}}+\omega_2\max\left[\frac{L^{p}_{\text{peak}}-L^{\text{bank},p}}{L^{\text{bank},p}},0\right]\right\} \tag{1}$$

s.t.

$$\frac{1}{2}[(I_{t-1}+I_t)-(R_{t-1}+R_t)]=\frac{1}{\Delta t}(S_t-S_{t-1}),\quad \text{for } t=1,2,\ldots,t_{III} \tag{2}$$

$$\left[\vec{I}_t,\overrightarrow{IL}_t\right]=\int_0^t f_{\text{runoff}}\left(\vec{P}_\tau\right)\,\mathrm{d}\tau,\ \text{for } t=1,2,\ldots,t_{III} \tag{3}$$

$$\vec{L}_t=f_{RIV}\left(\vec{L}_{t-1},\overrightarrow{IL}_t,\overrightarrow{IL}_{t-1},R_t,R_{t-1}\right),\ \text{for } t=1,2,\ldots,t_{III} \tag{4}$$

$$\begin{cases} I_{\text{peak}}=\max\ (I_\tau)_{\tau=1,2,\ldots,t_{III}} \\ R_{\text{peak}}=\max\ (R_\tau)_{\tau=1,2,\ldots,t_{III}} \\ L^{p}_{\text{peak}}=\max\ (L^{p}_\tau)_{\tau=1,2,\ldots,t_{III}} \end{cases} \tag{5}$$

$$h_t=f_{hv}(S_t),\ \text{for } t=1,\ldots,t_{III} \tag{6}$$

$$h_t\le h^{\max},\ \text{for } t=1,\ldots,t_{III} \tag{7}$$

$$R_t\le R^{\max}=g_{ff}(h_t),\ \text{for } t=1,\ldots,t_{III} \tag{8}$$

$$\begin{aligned} &cms\ \text{for}\ t=1,2,\ldots,t_I \\ &R_{t-1}\le R_t\le\max\,(I_\tau)_{\tau=1,2,\ldots,t}\ \text{for}\ t=t_I+1,\ldots,t_{II} \\ \{R_t\le 1850\ &\frac{R_t-R_{t-1}}{\Delta t}\le\max\left(\frac{I_\tau-I_{\tau-1}}{\Delta t}\right)_{\tau=2,3,\ldots,t}\ \text{for}\ t=t_I+1,\ldots,t_{II} \\ &R_t\le\min\left[R_{t-1},\max\,(I_\tau)_{\tau=1,2,\ldots,t}\right]\ \text{for}\ t=t_{II}+1,\ldots,t_{III} \end{aligned} \tag{9}$$

in which S_t and h_t are reservoir storage and water level at the time t; $S_{\max}$ and $h_{\max}$ are maximum reservoir storage and water level; S_{target} and h_{target} are targeted storage and water level; $S_{t_{III}}$ and $h_{t_{III}}$ are reservoir storage and water level after the typhoon and the flood period has ended; L^{p}_{peak} is the peak river stage at the downstream control point; $L^{\text{bank},p}$ is the top of levee at the downstream control point; I_t is the inflow to reservoir at time t; $\vec{P}_t$ is the precipitation recorded

in the watershed; I_{peak} is the peak inflow to the reservoir; R_t is the release of reservoir at time t; R_{peak} is the peak release of reservoir; R^{max} is the maximum release of floodway; and $\overrightarrow{IL}_t$ is the lateral inflow to the river. The function f_{RIV} is the governing equation of river simulation; the function f_{hv} is the transfer function of the reservoir water level (H) – storage (V) curve; and the function g_{ff} is the transfer function of the free flow rating curve.

Equations (1)–(9) showed the objective function and constraint functions in the OFOPM. The objective function, Equation (1), includes two objectives. The first objective is that the post typhoon reservoir water level should meet the targeted storage (S_{target}). That means the absolute difference between the storage at the end of the flood period ($S_{t_{III}}$) and targeted storage (S_{target}) should be as small as possible. The second objective follows Valeriano *et al.*'s (2010) idea that the flooding operation should allocate the quantity of peak flow into the spare volume of reservoir storage or river channel capacity. When the peak river stage is higher than the top of the levee, the damage downstream has already occurred and the reservoir storage should be used instead for the flood mitigation. The objective function uses the difference between the top of the levee $(L^{bank,p})$and peak river stage (L^p) to describe the downstream damage. To combine these two objectives, S_{target} and $L^{bank,p}$ are normalized and weighted with ω_1 and ω_2. The decision variable is the release of reservoir ($\vec{R}_t$) at one minute intervals.

Equations (2)–(6) are the equality constraints. Equation (2) ensures that the continuity equation is satisfied. The storage S equals the difference between inflow (I) and outflow (R). Equation (3) is a conceptual formulation of a runoff model. The inflow of reservoir ($\vec{I}_t$) and lateral flows of river ($\overrightarrow{IL}_t$) of the t-th time step are the total effects of precipitation from the beginning to the current time step. More detail of the runoff model is illustrated in the appendix (available online at http://www.iwaponline.com/nh/045/201.pdf). The downstream river hydraulic equation is shown in Equation (4). The HEC-RAS was used in this study to model the river hydraulics and then ANN was applied to replace HEC-RAS for further modeling works (see details in 'ANN for forecasting flood stage' section). The river stage is influenced by the previous river stage, reservoir release, and lateral inflow. The lateral inflow was described in the 'Calculation of surface runoff' section. Equation (5) calculates the peak inflow, release, and river stage at the downstream control point. Equation (6) is the reservoir water level (H) – storage (V) curve of Tseng-Wen Reservoir. Figure 2(a) shows the relationship between the reservoir water level (h_t) and storage (S_t).

Equations (7) and (8) are inequality constraints. To ensure the safety of the dam structure, Equation (7) describes the storage of the reservoir and it should be less than the maximum allowable storage. For the spillway, Equation (8) defines the maximum allowable spill by following the free flow rating curve (Figure 2(b)) which is a function of the reservoir water level (h_t).

Water Resources Agency (2011) published the Tseng-Wen Reservoir operation rules, which were divided into three steps. The three steps, illustrated in Figure 3, are (1) before flood, (2) before peak flow, and (3) after peak flow. Equation (9) shows the individual rule of release in each step. The details of the officially published operation rules are described as follows.

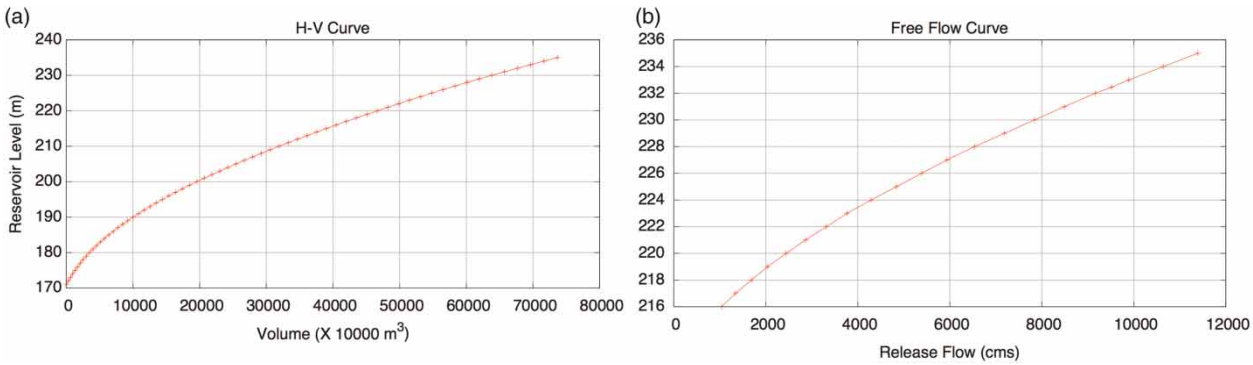

Figure 2 | The characteristic curve of Tseng-Wen Reservoir: (a) H-V curve; (b) free flow.

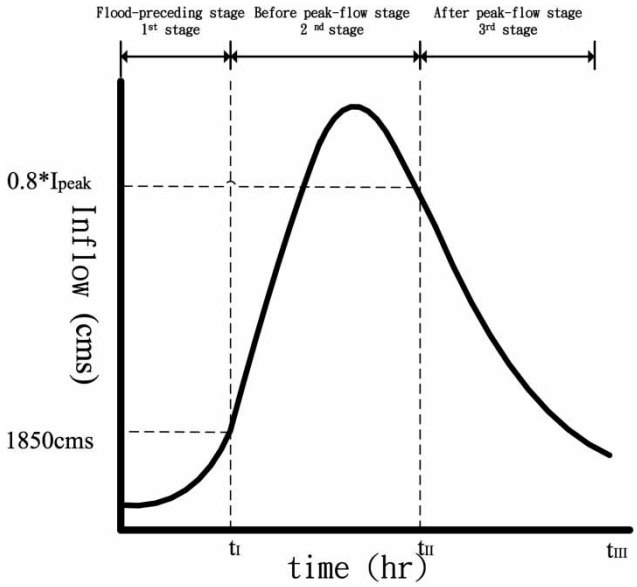

Figure 3 | The schematic of flooding operation rules.

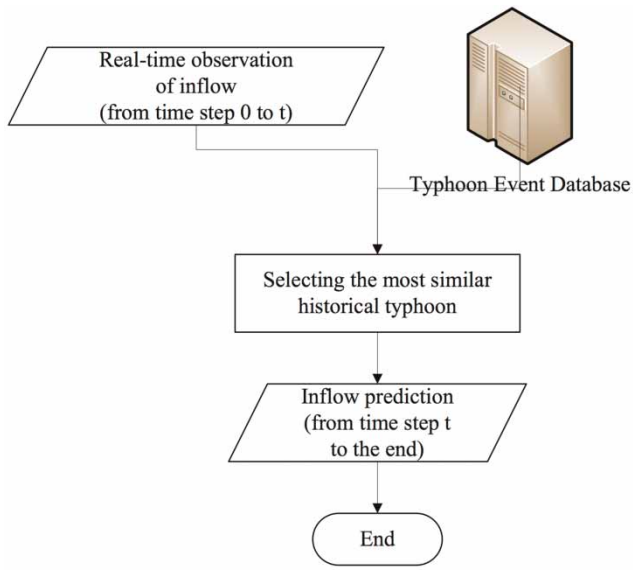

Figure 4 | The flowchart of real-time inflow forecasting.

Step 1. Before flood (from t_0 to t_I): The duration of the first step is defined by the inflow (I_t). If the inflow is less than 1,850 cubic meters per second (cms), it is in the first step. During this step, the reservoir could release and draw down the water level to increase the empty volume for the future flood. The constraint of this step is that the release should not be greater than 1,850 cms.

Step 2. Before peak flow (from t_I to t_{II}): The second step is that the inflow (I_t) to Tseng-Wen Reservoir is greater than 1,850 cms. There are two constraints: (1) the release (R_t) cannot be larger than the maximum inflow or smaller than the release of the previous time step; (2) the increase rate of the release cannot be larger than the increase rate of inflow.

Step 3. After peak flow (from t_{II} to t_{III}): When the inflow reaches 80% of the peak inflow (I_{peak}), there are two constraints: (1) the release (R_t) is not larger than the peak inflow (I_{peak}); (2) the release (R_t) is not larger than the release at the previous moment (R_{t-1}).

Typhoon event database

This study built a database composed of historical records from 40 typhoon events. The database was used for the prediction of future inflow for the real-time operation. Figure 4 shows the flowchart of inflow forecasting. At time t, observed inflows were retrieved from the gauging station. The comparison between real-time observation and historical records can be automatically computed.

The comparison is based on an index, root-mean-squared-error (RMSE, shown as Equation (10)). I_τ^{RT} is the inflow quantity obtained from the gauging station of a real-time system. $I_\tau^{DB,k}$ is the inflow quantity of the k-th typhoon recorded in the database. In Equation (10), the index should sum the temporary differences from the beginning of the typhoon to the current time step (t). A smaller RMSE_t^k means that the k-th historical typhoon is more similar. The historical inflows of the k-th typhoon are assigned as the forecasting of the current typhoon. The length of forecast horizon is equal to the length of the k-th typhoon.

$$\min_k \mathrm{RMSE}_t^k = \frac{1}{t}\sum_{\tau=1}^{t}\left(I_\tau^{RT} - I_\tau^{DB,k}\right)^2 \tag{10}$$

APPLICATION OF RTFOM IN THE TSENG-WEN RESERVOIR REAL-TIME OPERATION

Figure 5 showed the Tseng-Wen River system: upstream linking to Tseng-Wen Reservoir, downstream linking to the southern Taiwan Strait, and Houjiue River, Tsailiau River,

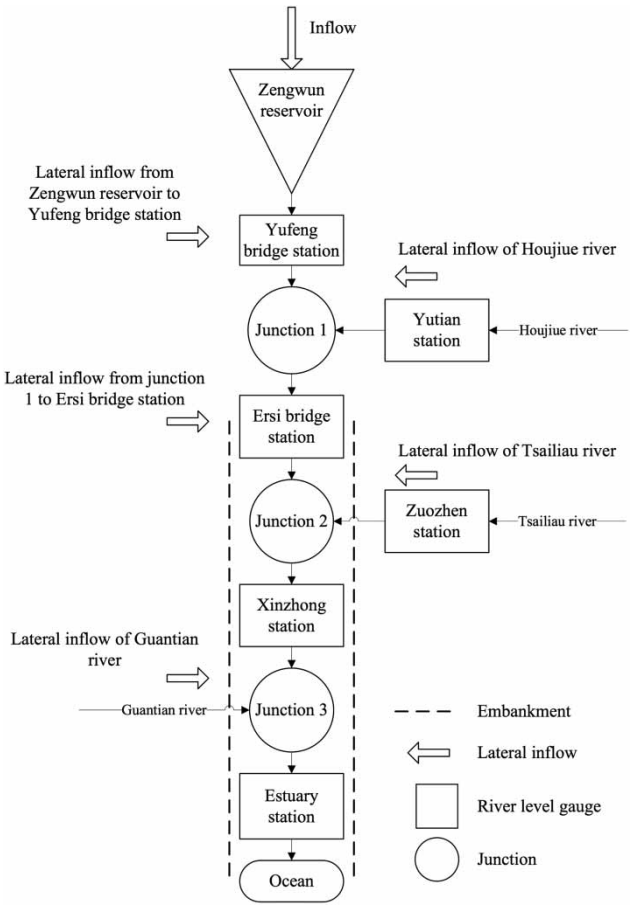

Figure 5 | The Tseng-Wen River system.

Guantian River along the side providing the lateral flow. Using the surface runoff model, the lateral inflow was calculated and provided into HEC-RAS to simulate Tseng-Wen River (see details in 'Calculation of surface runoff' section). Then the ANN is applied as a substitution for HEC-RAS in Tseng-Wen River modeling (see details in 'ANN for forecasting flood stage' section). The 'Application of OFOPM and RTFOM in Tseng-Wen Reservoir flooding operation' section describes the results of applying OFOPM and RTFOM. Historical records of six typhoons including Sepat (2007), Krosa (2007), Kalmaegi (2008), Fung-wong (2008), Sinlaku (2008), and Jangmi (2008) are applied for the process of calibration, verification and operation of the proposed model. The information for historical typhoons is listed in Table 1. The lengths of these typhoons vary from 68 to 110 hours. The peak inflows of the reservoir vary from 1,748 to 6,939 cms.

Table 1 | The table of information for historical typhoons

Name	Duration	Length (hr)	Initial Reservoir Level (m)	Peak Inflow (cms)
Sinlaku	2008/9/12–2008/9/16	68	221.7	4251
Sepat	2007/8/16–2007/8/22	110	210.1	1748
Krosa	2007/10/5–2007/10/9	86	226.4	5784
Jangmi	2008/9/27–2008/10/1	87	225.5	4424
Fung-wong	2007/7/26–2007/7/30	78	223.2	2639
Kalmaegi	2007/7/17–2007/7/21	98	207.6	6939

Calculation of surface runoff

There are five surface runoff sources ($\overrightarrow{IL}_t$) into the Tseng-Wen River (Figure 5). Three of the sources are from the major tributaries of Tseng-Wen River called the Houjiue River, the Tsailiau River, and the Guantian River. The remaining two lateral inflows are from the surface runoff upstream of Ersi Bridge. The Tseng-Wen River is upstream of Ersi Bridge, which has no levee along the side to prevent the surface runoff flowing into the mainstream. The two areas without a levee along the side are between Tseng-Wen Reservoir and Yufeng Bridge and between Yufeng Bridge and Ersi Bridge. Surface runoff contributes inflow to the river channel which may impact the decision of upstream reservoir operation. These five sources of surface runoff necessarily need to be considered for flooding operation. In addition, the inflow ($\vec{I}_t$) to Tseng-Wen Reservoir from upstream of the watershed also needs to be estimated. This study applied kinematic-wave based geomorphic instantaneous unit hydrograph (KW-GIUH) (Lee & Yen 1997; Cao *et al.* 2010) to model all the surface runoffs that were mentioned above (further detail of KW-GIUH is introduced in the appendix, available online at http://www.iwaponline.com/nh/045/201.pdf). The KW-GIUH model is calibrated by the case of Sinlaku and five other cases verify the accuracy of the well-calibrated KW-GIUH model.

ANN for forecasting flood stage

This study applied the unsteady HEC-RAS model to estimate the peak flood stage in the river. The information required by HEC-RAS is river cross sections, Manning's n, and

boundary conditions upstream and downstream of the river. This study compared the modeling results with observed stage levels at Xinzhong station for the six cases including Sepat, Krosa, Kalmaegi, Fung-wong, Sinlaku, and Jangmi. The stage comparisons are presented in Figure 6. The modeling results and observed stage have the same pattern for all the cases except for Krosa. For Krosa, the occurred time of the peak flow in the HEC-RAS simulation is several hours earlier than the one in the observed data. Table 2 shows the difference in peak stage was less than 0.5 m in all cases and the correlation coefficient was great than 0.97. The model satisfactorily represents the stage at Tseng-Wen River. The model also shows a high risk of overtopping at Section 85 in between Tsailiau River and Xinzhong station due to the low top of the levee.

This study combines a river hydraulic model and an optimization model to provide efficient river hydraulic forecasting. A large number of modeling results of HEC-RAS were used to train the ANN flood forecasting model. After that, the ANN flood forecasting model replaced HEC-RAS to forecast the flood stage for the purpose of efficiency.

This study applies back propagation network to the ANN model which is one kind of supervised learning that needs inputs and outputs. The flow rate at five locations serves as the input to the model at time t and $t-1$. The five locations are the Yufeng Bridge, Ersi

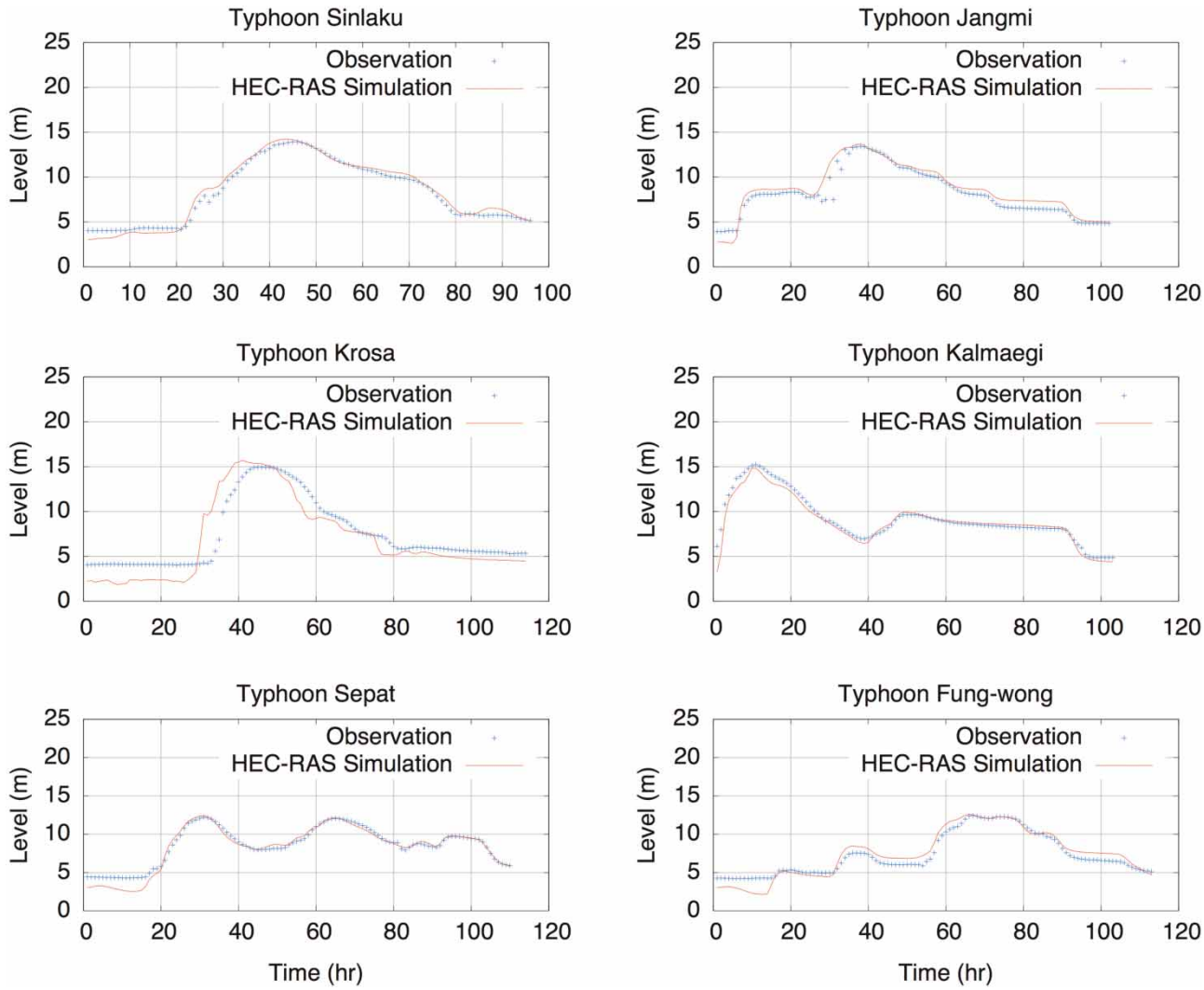

Figure 6 | The comparison modeling result and observed runoff at Yufeng Bridge station.

Table 2 | The comparison of modeling results and observed river stage at Section 85

	Correlation coefficient	Root mean square error m	Difference in peak flow m
Sinlaku	0.99	0.52	0.3
Sepat	0.98	0.33	0.21
Krosa	0.98	0.8	0.43
Jangmi	0.97	0.82	0.28
Fung-wong	0.98	0.68	0.16
Kalmaegi	0.98	0.58	0.38

Bridge, Houjiue River, Tsailiau River, and Guantian River. The river stage at high risk of overtopping location, which is between Tsailiau River and Xinzhong station (downstream cross section No. 85), was selected as the output. Shown as Figure 7, there was a hidden layer with four neurons in the model.

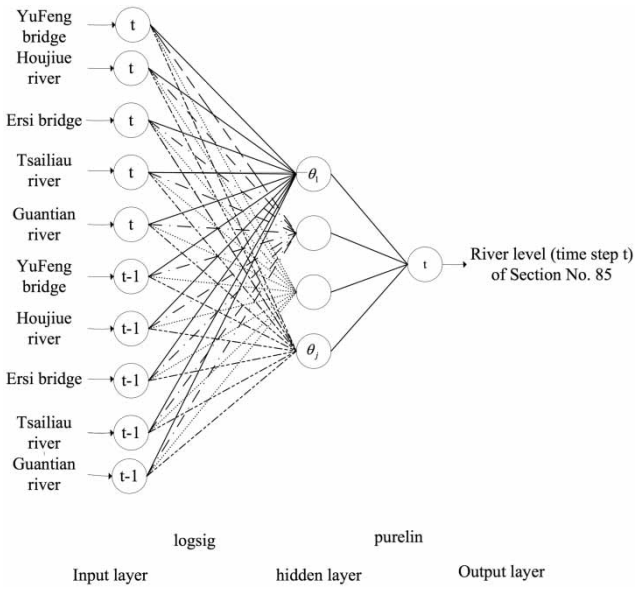

Figure 7 | ANN forecasting river stage model.

The study used four typhoons including Sinlaku, Sepat, Fung-wong, and Krosa for training the model. Two typhoons, Kalmaegi and Jangmi, were used to verify the model. Figure 8 shows the comparisons of HEC-RAS and the ANN flood forecasting model for the cases of Sinlaku and Jangmi. Both results show a similar pattern. The correlation coefficient was 0.98 and the difference at peak stage was approximate 0.51 m. The details are shown in Table 3.

Application of OFOPM and RTFOM in Tseng-Wen Reservoir flooding operation

In the formulation of OFOPM (from Equations (1)–(9)), several parameters and variables should be assigned and calculated. The values of each parameter are listed in Table 4. The target storage of reservoir after flooding operation (S^{target}) is defined as the upper bound of the operation rule curves announced by Taiwan government and the value of S^{target} is 54,828.9 m^3. The top level of the levee at Xinzhong station ($L^{\text{bank},p}$) is 15.13 m. These two parameters are used to normalize the two sub-objective terms in Equation (1). Because the two sub-objective terms have been normalized, the weights (ω_1 and ω_2) are simultaneously assigned as 1.0.

The variables of t_I, t_{II} and t_{III} for each of the simulations which separate the entire processes of typhoons into three steps are determined from the historical records of each typhoon. The variable of S_0 which is the initial storage of the reservoir is assigned depending on the historical records of each typhoon. The quantities of $\vec{I}_t$ and $\overrightarrow{IL}_t$ are calculated

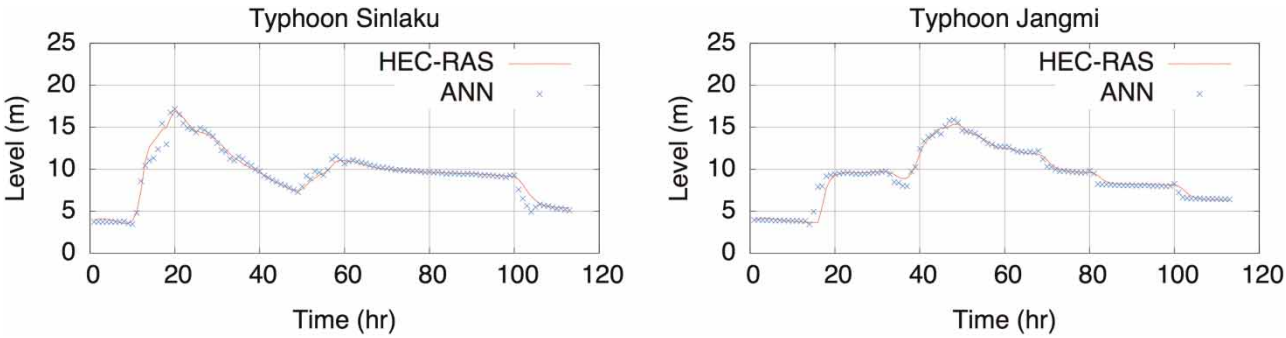

Figure 8 | The comparison of HEC-RAS and ANN forecasting river stage model for river stage at Section 85.

Table 3 | The comparison of HEC-RAS and ANN flood forecasting model at Section 85

	Correlation coefficient	Root mean square error m	Difference in peak flow m
Kalmaegi	0.98	0.55	0.25
Jangmi	0.98	0.58	0.51

Table 4 | The table of parameter and variable assignment for the flooding operation of Tseng-Wen Reservoir

Parameter	Value	Parameter	Value
S^{target}	54,828.9 m^3	$L^{bank,p}$	15.13 m
ω_1	1.0	ω_2	1.0
t_I, t_{II} and t_{III}	Depend on the historical records of each typhoon		
S_0	Initial condition. Depends on the historical records of each typhoon		
$\vec{I}_t$ and $\overrightarrow{IL}_t$	Calculated by Equation (3)		
$\vec{L}_t$	Calculated by Equation (4)		
R_t	The decision variable of OFOPM		

by Equation (3) and the level ($\vec{L}_t$) is calculated by Equation (4). The reservoir release (R_t) is the decision variable which is optimally determined by OFOPM.

Based on six historical typhoons, including Sepat, Krosa, Kalmaegi, Fung-wong, Sinlaku, and Jangmi, the OFOPM and RTFOM have been applied to compare the performance of the proposed models with the performance of the practical operation. Because the OFOPM is a kind of planning model, the inflow information of entire typhoon periods should be assigned before solving the optimization of OFOPM. However, a real-time model is required to make the decision for the current time step based on the previous information obtained from the observation system. A numerical experiment is applied to simulate the real-time process. For the decision of the t-th time step, the operation of RTFOM is based on the previous information in the numerical experiment. The future quantities of inflow are predicted based on the typhoon event database mentioned in the 'Typhoon event database' section.

Figures 9 and 10 show the comparisons of the optimal operation for Typhoon Krosa and Sinlaku. Tables 5 and 6 list the comparisons for optimal operation between Sepat, Krosa, Kalmaegi, Fung-wong, Sinlaku, and Jangmi.

Figure 9 contains a comparison of Typhoon Krosa between the practical operation, OFOPM, and RTFOM. Since the initial water level was 226 m which was high for the OFOPM and RTFOM, both models released water at rate of 1,100 cms at the early period of the flood to increase available storage for the coming flood. In contrast, the practical operation did not release water from the reservoir. Therefore there was more available space for flood mitigation from the operations of OFOPM and RTFOM which reduced the peak flow. The peak inflow was 5,784 cms. The peak releases from the practical operation, OFOPM, and RTFOM were 4,850, 3,300 and 3,912 cms, respectively. The corresponding reductions compared with the inflow were 16.1, 42.9 and 32.3%. The OFOPM and RTFOM efficiently used the available storage in the reservoir to reduce the peak flood flow. The overtopping happened for all three operations for the downstream area. Compared with the practical operation, the OFOPM and RTFOM decreased the water levels by 0.6 and 0.4 m and decreased the flooding duration by 3 and 4 hours, respectively. This reduced the damage due to the flooding. In comparison with the targeted water level of 227 m, the water levels at the end of the flood period for the practical operation, OFOPM, and RTFOM were 228.1, 227, and 227.1 m, respectively. See Figure 10 for the comparison of Typhoon Sinlaku. The initial water level was 221 m. Hence OFOPM and RTFOM released water at a rate of 650 cms. The practical operation did not release any water and OFOPM and RTFOM efficiently reduced the peak flow. The peak inflow was 4,251 cms. The peak releases from the practical operation, OFOPM, and RTFOM were 2,840, 1,737, and 2,239 cms respectively. The corresponding reductions compared with the inflow were 33.2, 59.1 and 47.3%. The overtopping still occurred for all three operations for the downstream area. However, the OFOPM and RTFOM decreased the flooding duration by 5 and 3 hours, respectively, when compared with the practical operation. In addition, the water levels at the end of flood period for the practical operation, OFOPM, and RTFOM were 226, 227, and 227.7 m. Compared with the practical operation, the OFOPM and RTFOM were closer to the targeted level of 227 m.

In Table 3, all of the practical operation, OFOPM, and RTFOM mitigated the impact of flooding by using the

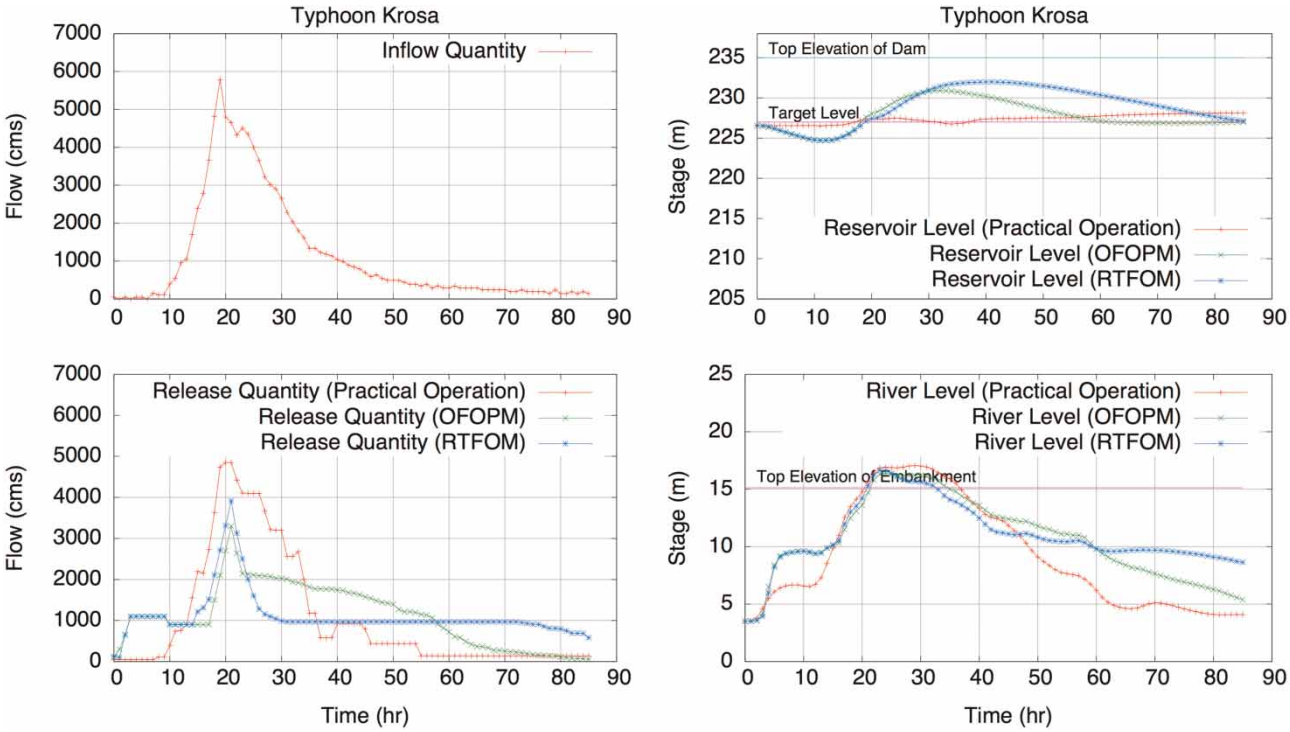

Figure 9 | The comparison of release for Typhoon Krosa between practical operation, OFOPM, and RTFOM.

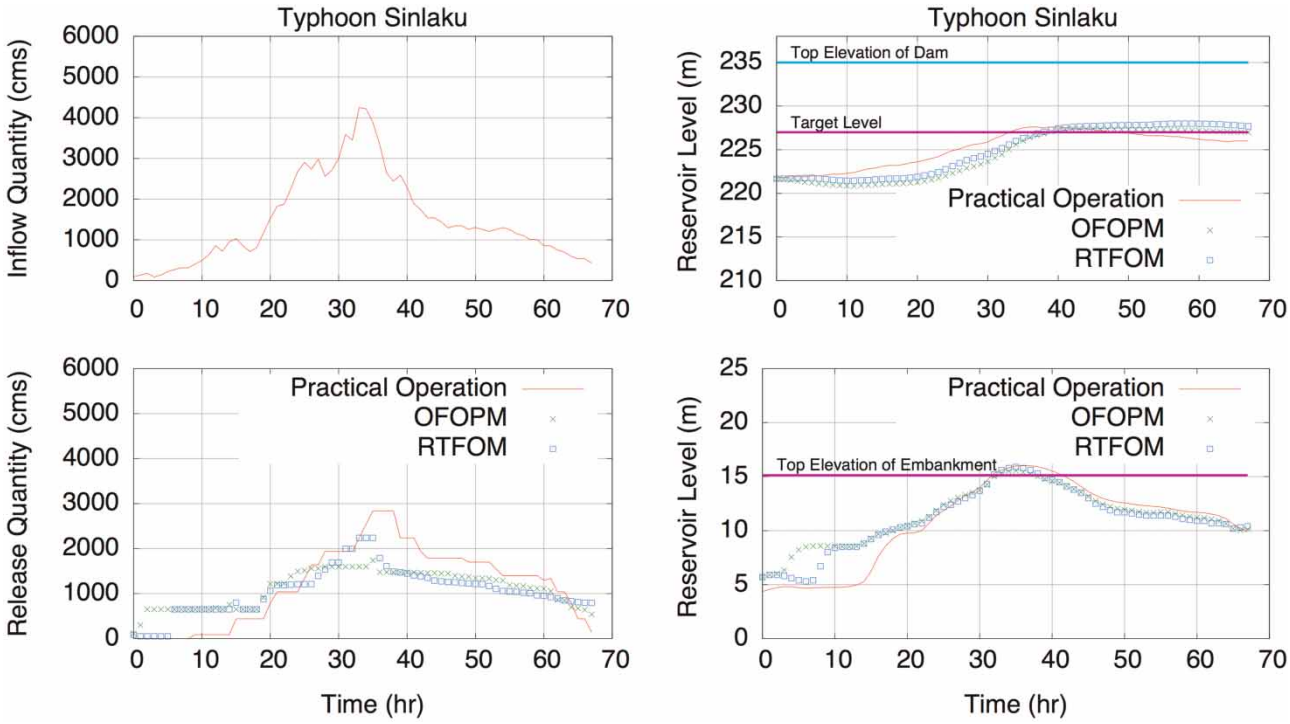

Figure 10 | The comparison of release for Typhoon Sinlaku between practical operation, OFOPM, and RTFOM.

Table 5 | The comparison of peak flow rate between practical operations, OFOPM, and RTFOM

			Practical operations		OFOPM		RTFOM	
	Initial water level[b]	Inflow[a]	Release[a]	Flood reduction[a]	Release[a]	Flood reduction[a]	Release[a]	Flood reduction[a]
Krosa	226.6	5784	4850	934	3300	2,484 (+1550)[c]	3913	1,871 (+937)[c]
Jangmi	225.5	4424	1940	2484	1577	2,847 (+363)[c]	1865	2,559 (+75)[c]
Fung-wong	223.2	2639	1550	1089	2163	476 (+613)[c]	1404	1,235 (+146)[c]
Sinlaku	221.8	4251.1	2840	1411	1737	2,513 (+1103)[c]	2239	2,011 (+601)[c]
Sepat	210.5	2854	1310	1544	566	2,288 (+744)[c]	1094	1,760 (+216)[c]
Kalmaegi	207.6	6939	700	6239	440	6499 (+260)[c]	440	6,499 (+260)[c]

[a]Unit: cms.
[b]Unit: m.
[c]Difference with the practical operation.

Table 6 | Comparisons of control node at the downstream river between the practical operation, OFOPM, and RTFOM

	Practical operation		OFOPM		RTFOM	
	Peak stage[a]	Overtopping duration[b]	Peak stage[a]	Overtopping duration[b]	Peak stage[a]	Overtopping duration[b]
Krosa	17.05[c]	16	16.4[c]	13	16.65[c]	12
Jangmi	15.38[c]	2	15.13	0	15.33[c]	2
Fung-wong	13.97	0	14.4	0	13.49	0
Sinlaku	16.02[c]	10	15.56[c]	5	15.9[c]	7
Sepat	13.73	0	14.2	0	14.26	0
Kalmaegi	16.93[c]	5	17[c]	5	17.1[c]	5

[a]Unit: meter.
[b]Unit: hour.
[c]The river level is higher than the top of levee (15.13 m).

available storage of Tseng-Wen Reservoir. For the practical operation, the reservoir water level before flood had an impact on the flood mitigation. For the Typhoon Kalmaegi and Krosa, the water levels before flood were 207.6 and 226.6 m. The 19 m difference in the water level had a significant impact on the available reservoir storage. This available storage is the reason for the difference in the flood mitigation values of 6,239 and 934 cms.

Given reliable inflow information, OFOPM provided the best operating results (Table 5). Compared with the practical operation, OFOPM efficiently utilized the available reservoir storage and reduced the peak flow by around 260–1,550 cms. RTFOM reduced the peak flow by around 75–937 cms in comparison with the practical operation. Comparing the source of inflow given to OFOPM and RTFOM, observed inflows were used in the OFOPM and similar inflows from the typhoon event database were selected in the RTFOM. The former has no error and theoretically OFOPM can obtain the global optimal. These results indicate that

the accuracy of inflow forecast impacts the results significantly.

Table 6 compared the peak stage and flooding duration at downstream control nodes with the practical operation, OFOPM, and RTFOM. The levee top at the control node (Section 85) was 15.13 m. For the practical operation, there were four typhoons including Krosa, Jangmi, Sinlaku, and Kalmaegi that resulted in downstream overtopping with a flooding duration of 16, 2, 10, and 5 hours. As mentioned before, Tseng-Wen Reservoir efficiently reduced the peak flow by utilizing its available reservoir storage. Despite this efficient reservoir storage, the lateral inflows from other watersheds still caused downstream flooding. For OFOPM, there were three typhoons including Krosa, Sinlaku, and Kalmaegi that resulted in downstream flooding. OFOPM prevented flooding in the Typhoon Jangmi. For Krosa, Sinlaku, and Kalmaegi, OFOPM reduced the downstream water level by approximately 10 cm and shortened the flooding duration in the typhoon events by as much as 5 hours. OFOPM showed significantly the advantage of disaster mitigation.

CONCLUSION

The performance of the RTFOM model has been checked with six historical events. By comparing with the practical operations carried out by the experts, the RTFOM model produced similar or even improved results in flood reduction, downstream damage mitigation, and reservoir storage at the end of the flood period.

The reservoir water level before flooding impacts the flooding operation significantly. Lowering the level decreases the peak flood and increases the efficiency of the flooding operation. On the contrary, retaining a higher water level before flooding results in less flood mitigation.

This study shows that the spare volume of Tseng-Wen Reservoir can significantly decrease the peak flow during a flood event in the Tseng-Wen River. However, contributions from other laterial sources, and surface runoff from other watersheds also impact the main stream. During major storms or typhoons, the downstream area would possibly encounter the flooding due to the free surface runoff even though the upstream reservoir already mitigates the peak flow.

The ANN flood forecasting model developed in this study correctly predicted the flow rate and river stage at the downstream. Compared with the HEC-RAS model, the model provided acceptable accuracy and saved a lot of calculation time, which gives the operator more lead time to response the flood.

The RTFOM in this study forecasted future inflow to the reservoir by retrieving similar observed past inflows from the typhoon event database. This database contained information about the historical observed inflows only. Recommendations for future study are to consider the typhoon path, satellite images, gauged rainfall, and the product obtained from Quantitative Precipitation Estimation and Segregation Using Multiple Sensors, abbreviated as QPESUM. These additional sources of data will improve the efficiency and accuracy of forecasting inflow and decrease the uncertainty of real-time operation.

ACKNOWLEDGEMENT

The authors would like to thank the National Science Council of China (Taiwan), which supported this research under contract NSC 99-2218-E-006-240.

REFERENCES

Ahmed, E.-S. M. S. & Mays, L. W. 2013 Model for determining real-time optimal dam releases during flooding conditions. *Natural Hazards* **65** (3), 1849–1861.

Alemu, E. T., Palmer, R. N., Polebitski, A. & Meaker, B. 2010 Decision support system for optimizing reservoir operations using ensemble streamflow predictions. *Journal of Water Resources Planning and Management* **137** (1), 72–82.

Cao, S., Lee, K. T., Ho, J., Liu, X., Huang, E. & Yang, K. 2010 Analysis of runoff in ungauged mountain watersheds in Sichuan, China using kinematic-wave-based GIUH model. *Journal of Mountain Science* **7** (2), 157–166.

Chang, F. & Chen, L. 1998 Real-coded genetic algorithm for rule-based flood control reservoir management. *Water Resources Management* **12** (3), 185–198.

Chang, L.-C., Chen, Y.-W. & Yeh, M.-S. 2009a Optimizing system capacity expansion schedules for groundwater supply. *Water Resources Research* **45**, W07407.

Chang, L.-C., Ho, C.-C. & Chen, Y.-W. 2009b Applying multiobjective genetic algorithm to analyze the conflict among different water use sectors during drought period. *Journal of Water Resources Planning and Management* **136** (5), 539–546.

Chang, L.-C., Chang, F.-J., Wang, K.-W. & Dai, S.-Y. 2010 Constrained genetic algorithms for optimizing multi-use reservoir operation. *Journal of Hydrology* **390** (1), 66–74.

Delgoda, D. K., Saleem, S. K., Halgamuge, M. N. & Malano, H. 2013 Multiple model predictive flood control in regulated river systems with uncertain inflows. *Water Resources Management* **27** (3), 765–790.

Halff, A., Halff, H. & Azmoodeh, M. 1993 Predicting runoff from rainfall using neural networks. In: Kuo, C. Y. (ed.), Proceedings of the Symposium sponsored by the Hydraulics Division of ASCE, Engineering Hydrology, San Francisco, CA, July 25–30 (1993), pp. 76–765.

Hınçal, O., Altan-Sakarya, A. B. & Ger, A. M. 2011 Optimization of multireservoir systems by genetic algorithm. *Water Resources Management* **25** (5), 1465–1487.

Holland, J. H. 1975 *Adaptation in Natural and Artificial Systems: An Introductory Analysis with Applications to Biology, Control, and Artificial Intelligence*. University of Michigan Press, Ana Arbor, Michigan.

Hsu, N. & Wei, C. 2007 A multipurpose reservoir real-time operation model for flood control during typhoon invasion. *Journal of Hydrology* **336** (3–4), 282–293.

Labadie, J. W. 2004 Optimal operation of multireservoir systems: State-of-the-art review. *Journal of Water Resources Planning and Management-ASCE* **130** (2), 93–111.

Lee, K. T. & Yen, B. C. 1997 Geomorphology and kinematic-wave-based hydrograph derivation. *Journal of Hydraulic Engineering* **123** (1), 73–80.

Loke, E., Warnaars, E., Jacobsen, P., Nelen, F. & do Cèu Almeida, M. 1997 Artificial neural networks as a tool in urban storm drainage. *Water Science and Technology* **36** (8), 101–109.

Lorrai, M. & Sechi, G. 1995 Neural nets for modelling rainfall-runoff transformations. *Water Resources Management* **9** (4), 299–313.

Malekmohammadi, B., Zahraie, B. & Kerachian, R. 2010 A real-time operation optimization model for flood management in river-reservoir systems. *Natural Hazards* **53** (3), 459–482.

Mays, L. W. & Tung, Y.-K. 2002 *Hydrosystems Engineering and Management*. Water Resources Publication, Littleton, Colorado.

Nash, S. G. & Sofer, A. 1996 *Linear and Nonlinear Programming*, Vol. 692. McGraw-Hill, New York.

Needham, J. T., Watkins, D. W., Lund, J. R. & Nanda, S. K. 2000 Linear programming for flood control in the IOWA and Des Moines rivers. *Journal of Water Resources Planning and Management-ASCE* **126** (3), 118–127.

Niewiadomska-Szynkiewicz, E., Malinowski, K. & Karbowski, A. 1996 Predictive methods for real-time control of flood operation of a multireservoir system: Methodology and comparative study. *Water Resources Research* **32** (9), 2885–2895.

Sajikumar, N. & Thandaveswara, B. 1999 A non-linear rainfall–runoff model using an artificial neural network. *Journal of Hydrology* **216** (1), 32–55.

Tayfur, G. & Singh, V. 2006 ANN and fuzzy logic models for simulating event-based rainfall-runoff. *Journal of Hydraulic Engineering* **132**, 1321.

Unver, O. & Mays, L. 1990 Model for real-time optimal flood control operation of a reservoir system. *Water Resources Management* **4** (1), 21–46.

Valeriano, O., Koike, T., Yang, K., Graf, T., Li, X., Wang, L. & Han, X. 2010 Decision support for dam release during floods using a distributed biosphere hydrological model driven by quantitative precipitation forecasts. *Water Resources Research* **46** (10), W10544.

Water Resources Agency 2011 Operation directions for Tseng-Wen reservoir. Technical report in Taiwan, Water Resources Agency, Ministry of Economic Affairs of Taiwan (ROC).

Wei, C. & Hsu, N. 2009 Optimal tree-based release rules for real-time flood control operations on a multipurpose multireservoir system. *Journal of Hydrology* **365** (3–4), 213–224.

Windsor, J. 1973 Optimization model for the operation of flood control systems. *Water Resources Research* **9** (5), 1219–1226.

Zhao, T., Zhao, J., Yang, D. & Wang, H. 2013 Generalized martingale model of the uncertainty evolution of streamflow forecasts. *Advances in Water Resources* **57**, 41–51.

First received 28 November 2012; accepted in revised form 22 October 2013. Available online 7 December 2013